

High-low frequency slaving and regularity issues in the 3D Navier-Stokes equations

J. D. Gibbon¹

Department of Mathematics, Imperial College London, SW7 2AZ, UK

Abstract

The old idea that an infinite dimensional dynamical system may have its high modes or frequencies slaved to low modes or frequencies is re-visited in the context of the 3D Navier-Stokes equations. A set of dimensionless frequencies $\{\tilde{\Omega}_m(t)\}$ are used which are based on L^{2m} -norms of the vorticity. A closure is assumed that suggests that the $\tilde{\Omega}_m$ ($m > 1$) are slaved to $\tilde{\Omega}_1$ (the global enstrophy) in the form $\tilde{\Omega}_m = \tilde{\Omega}_1 \mathcal{F}_m(\tilde{\Omega}_1)$. This is shaped by the constraint of two Hölder inequalities from which emerges a form for \mathcal{F}_m which has been observed in previous numerical Navier-Stokes and MHD simulations. When written as a phase plane in a scaled form, this relation is parametrized by a function $\lambda(t) \geq 1$, where curves of constant λ form the boundaries between tongue-shaped regions. In regions where $\lambda \geq 2.5$ and $1 \leq \lambda \leq 2$ the Navier-Stokes equations are shown to be regular: numerical simulations appear to lie in the latter region. Only in the central region $2 < \lambda < 2.5$ has no proof of regularity been found. Given that the closure is a kinematic relation, an application of this idea to data assimilation for more general systems is suggested.

Dedicated to the memory of David Broomhead (1950 – 2014)

1 Introduction

1.1 Historical background

A generation ago a recurrent theme in studies in infinite dimensional dynamical systems was the idea that a small subset of low modes or coherent states might conceivably control the dynamics by slaving the higher modes to this subset. Having originally emerged from earlier work on centre manifolds in studies in ordinary differential equations (Broomhead, Indik, Newell and Rand (1991), Guckenheimer and Holmes (1997), Holmes, Lumley and Berkooz (1996)), such ideas obviously have lasting appeal, particularly for those who work in turbulent fluid flows where the number of degrees of freedom are so large that resolved computations at realistic Reynolds numbers are hard to achieve: see Moin and Mahesh (1998), Donzis, Young and Sreenivasan (2008), Pandit, Perlekar and Ray (2009), Ishihara, Gotoh and Kaneda (2009), Kerr (2012, 2013) and Schumacher, Scheelb, Krasnov, Donzis, Yakhov and Sreenivasan (2014). For PDEs there also emerged a parallel and closely related body of work on global attractors and inertial manifolds, which aimed to prove the finite dimensionality of the system in question in some specified sense: Foias, Sell and Temam (1988), Titi (1990), Foias and Titi (1991), Robinson (1996), Foias, Manley, Rosa and Temam (2001). Some success was achieved for the one-dimensional Kuramoto-Sivashinsky equation where an inertial manifold was proved to exist (Foias, Jolly, Kevrekidis, Sell and Titi (1988)). Further success was also achieved for the 2D incompressible Navier-Stokes equations where a global attractor was shown to exist with a sharp estimate for its dimension (Constantin, Foias and Temam (1988)), with further estimates on the number of determining modes and nodes: see Foias and Prodi (1967), Foias and Temam (1984), Jones and Titi (1993), Olson and Titi (2003), Farhat, Jolly and Titi (2014).

The aim of this paper is to revisit the low/high mode idea in a new way in the context of the open question of the global regularity of the incompressible 3D Navier-Stokes equations

$$\mathbf{u}_t + \mathbf{u} \cdot \nabla \mathbf{u} = \nu \Delta \mathbf{u} - \nabla p + \mathbf{f}(\mathbf{x}), \quad \operatorname{div} \mathbf{u} = \operatorname{div} \mathbf{f} = 0, \quad (1.1)$$

¹j.d.gibbon@ic.ac.uk and www2.imperial.ac.uk/~jdg

with periodic boundary conditions on a cube of volume $\mathcal{V} = [0, L]_{per}^3$. The body force $\mathbf{f}(\mathbf{x})$ is taken to be L^2 -bounded and centred around a length scale ℓ in the manner described by Doering and Foias (2002). The two dimensionless numbers corresponding to the forcing and the system response to it are respectively given by the Grashof and Reynolds numbers

$$Gr = \frac{\ell^{3/2} \|\mathbf{f}\|_2}{\nu^2} \quad Re = \frac{\ell U_0}{\nu} \quad (1.2)$$

where $U_0^2 = L^{-3} \langle \|\mathbf{u}\|_2^2 \rangle$ with $\|\cdot\|_2$ representing the L^2 -norm and $\langle \cdot \rangle$ a time average.

1.2 A high-low frequency slaving closure

Given the open nature of the existence and uniqueness question for solutions of the 3D Navier-Stokes equations, regularity analyses have always been based on an assumption of some type. The main one has been that the velocity field is assumed to remain bounded in some function space, the best being the $u \in L^3(\mathcal{V})$ result of Escauriaza, Seregin and Sverák (2003). An alternative computational approach has been to discuss low modes in terms of coherent states by projecting onto special selections of Fourier-Galerkin modes (Broomhead, Indik, Newell and Rand (1991), Holmes, Lumley and Berkooz (1996))

Here we break with both of these traditions and instead introduce a set of time dependent frequencies or inverse time scales (or ‘modes’)

$$\{\Omega_1(t), \Omega_2(t), \dots, \Omega_m(t)\}, \quad (1.3)$$

based on L^{2m} -norms of the three-dimensional vorticity field $\boldsymbol{\omega}(\mathbf{x}, t)$ with the dimension of a frequency

$$\Omega_m(t) = \left(L^{-3} \int_{\mathcal{V}} |\boldsymbol{\omega}|^{2m} dV \right)^{1/2m}. \quad (1.4)$$

If $\boldsymbol{\omega}$ is the Navier-Stokes vorticity then $\Omega_1(t)$ is related to the global enstrophy and the $\Omega_m(t)$ are higher moments, all of which are assumed to exist. The set (1.3) would be widely spread if the vector field $\boldsymbol{\omega}(\mathbf{x}, t)$ is strongly intermittent, whereas they would be squeezed closely together if $\boldsymbol{\omega}$ is mild in behaviour. Multiplication by the inverse of the constant frequency $\varpi_0 = \nu L^{-2}$ produces a non-dimensional set $\tilde{\Omega}_m = \varpi_0^{-1} \Omega_m$.

The first step is to postulate a high/low frequency closure relating $\tilde{\Omega}_m$ to lower frequencies

$$\tilde{\Omega}_m = F_m(\tilde{\Omega}_1, \tilde{\Omega}_2, \dots, \tilde{\Omega}_n), \quad 1 \leq n < m. \quad (1.5)$$

The form of this closure must be constrained and shaped by the fact that $\tilde{\Omega}_m$ must not only satisfy Holder’s inequality

$$\tilde{\Omega}_1 \leq \dots \leq \tilde{\Omega}_m \leq \tilde{\Omega}_{m+1} \leq \dots \quad (1.6)$$

but it must also satisfy a triangular version Hölder’s inequality for $m > 1$ (see Appendix A)

$$\left(\frac{\tilde{\Omega}_m}{\tilde{\Omega}_1} \right)^{m^2} \leq \left(\frac{\tilde{\Omega}_{m+1}}{\tilde{\Omega}_1} \right)^{m^2-1}. \quad (1.7)$$

Given the two inequality constraints (1.6) and (1.7), we simplify the dependency of $\tilde{\Omega}_m$ to the first frequency $\tilde{\Omega}_1$ such that our closure in (1.5) is reduced to²

$$\tilde{\Omega}_m = \tilde{\Omega}_1 \mathcal{F}_m(\tilde{\Omega}_1). \quad (1.8)$$

²For a (strong) solution to exist requires the assumption that $\tilde{\Omega}_1(t)$, the H_1 -norm of the velocity field, is bounded : from this comes the result that all other $\tilde{\Omega}_m$ are bounded quantities. Strictly speaking, (1.8) is not a closure in the conventional sense used in turbulence modelling. Rather, it is an expression of how $\tilde{\Omega}_m$ can be related to $\tilde{\Omega}_1$, under the constraints (1.6) and (1.7). Nevertheless, we will continue to use the word ‘closure’ for convenience.

(1.6) and (1.7) then demand that \mathcal{F}_m must satisfy both $\mathcal{F}_m \geq 1$ and

$$\mathcal{F}_{m+1} \geq \mathcal{F}_m^{m^2/(m^2-1)}. \quad (1.9)$$

Then we consider a class of solutions of the form

$$\mathcal{F}_m = c_m \tilde{\Omega}_1^{p_m} \quad \text{where} \quad p_m = (\lambda(t) - 1)(m - 1)m^{-1}, \quad (1.10)$$

with $\lambda \geq 1$ taken as a potentially time-dependent parameter. The c_m are chosen to be constants such that

$$c_{m+1} \geq c_m^{m^2/(m^2-1)}, \quad (1.11)$$

and obviously require some initial c_{m_0} with a choice of $m_0 > 1$ to begin the iteration. Altogether we obtain the simple relation

$$\tilde{\Omega}_m = c_m \tilde{\Omega}_1^{1 + [(\lambda(t)-1)](\frac{m-1}{m})}. \quad (1.12)$$

This expresses the size of $\tilde{\Omega}_m$ relative to $\tilde{\Omega}_1$ through the function $\lambda(t) \geq 1$. Earlier work used a scaled version of the $\tilde{\Omega}_m$ (Gibbon (2011))

$$D_m = \tilde{\Omega}_m^{\alpha_m} \quad \text{with} \quad \alpha_m = \frac{2m}{4m-3}, \quad (1.13)$$

which were shown to have bounded long-time averages $\langle D_m \rangle \leq c Re^3$. Given that $\alpha_1 = 2$, the first of these $\langle D_1 \rangle \leq c Re^3$ is just the well-known result that the time average of the global enstrophy is a bounded quantity. The origin of the α_m -scaling in (1.13) comes from symmetry considerations. When (1.12) is re-written in the D_m -format of (1.13) the following relation is obtained

$$D_m = c_{1,m} D_1^{A_{m,\lambda}} \quad \text{with} \quad A_{m,\lambda} = \frac{(m-1)\lambda(t) + 1}{4m-3}. \quad (1.14)$$

It is worth remarking at this point that in a set of 3D Navier-Stokes numerical simulations described in Donzis *et al.* (2013) and Gibbon *et al.* (2014), plots of the maxima in time of $\ln D_m / \ln D_1$ fitted the $A_{m,\lambda}$ in (1.14) with $c_{1,m} = 1$; the accuracy of the fit lay within 5%. The corresponding fixed values of λ lay in the range $1.15 \leq \lambda \leq 1.5$. These numerical simulations were: (i) a $1024^2 \times 2048$ decaying calculation with anti-parallel initial conditions at about $Re_\lambda \sim 400$ based on work reported in Kerr (2012, 2013); (ii) a forced and a decaying $(512)^3$ pair of simulations at about $Re_\lambda \sim 250$ – see Gibbon *et al.* (2014); (iii) data from a large-scale statistically steady simulation $(4096)^3$ simulation on 10^5 processors at $Re_\lambda \approx 1000$, reported in Donzis *et al.* (2008, 2010) and Yeung, Donzis and Sreenivasan (2012). In addition to these, (1.14) has also been seen in a set of 3D-MHD simulations in similar circumstances to those performed for the Navier-Stokes equations: see Gibbon *et al.* (2015).

1.3 Data assimilation

Putting aside the α_m -scaling in the relation (1.13), which is specific to the Navier-Stokes equations, the relation between $\tilde{\Omega}_m$ and $\tilde{\Omega}_1$ in (1.12) is a kinematic result which is true for all bounded periodic functions ω under the closure (1.8) ($\lambda \geq 1$). No Navier-Stokes information has been used to derive it. Thus, any reliable data-set from a spatially periodic system could be analyzed in the following way:

1. Consider a 3D data-set $\omega(\mathbf{x}, t)$ with enough spatial points to construct the Ω_m .
2. Find a natural constant frequency ϖ_0 that will non-dimensionalize the Ω_m to create $\tilde{\Omega}_m$.
3. Plots of $\tilde{\Omega}_m$ versus $\tilde{\Omega}_1$ from (1.12) will yield a family convex curves for constant values of $\lambda \geq 1$, as in Fig. 1. The size and trajectory of $\lambda(t)$ will suggest the degree of intermittency of the data.

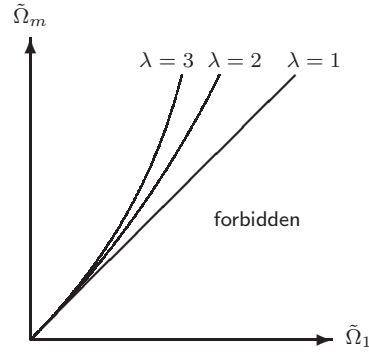


Figure 1: Plots of the convex curves \tilde{Q}_m versus \tilde{Q}_1 for $\lambda = 2, 3$ lying above the straight line $\lambda = 1$. As λ increases the \tilde{Q}_m spread more, corresponding to greater intermittency in the ω -field.

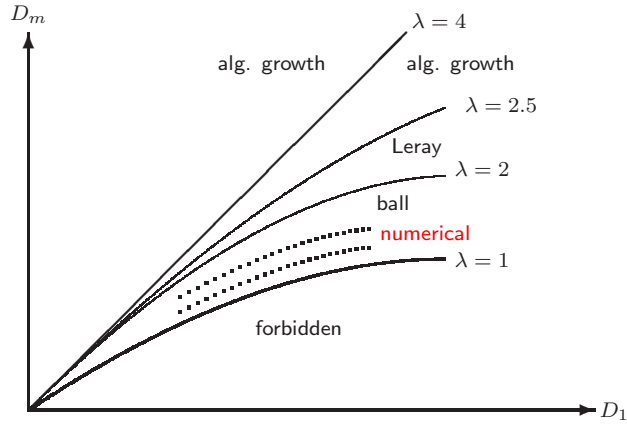


Figure 2: A cartoon in the $D_1 - D_m$ plane parametrized by λ : in the region $\lambda \geq 2.5$ the D_m undergo no more than algebraic growth with a restriction on (large) initial data for $2.5 \leq \lambda \leq 4$; in the region $2 < \lambda < 2.5$ only Leray's weak solutions are known to exist with the only control over D_m being the bounded long time averages $\langle D_m \rangle < \infty$; at $\lambda = 2$ the bound on D_1 grows exponentially in time; in the region $1 \leq \lambda < 2$ the D_m lie within an absorbing ball. The dotted curves represent the approximate regions of the maxima in the numerical simulations reported in Donzis *et al.* (2013) and Gibbon *et al.* (2014). The region below the curve $\lambda = 1$ is forbidden as Hölder's inequality is violated there.

2 Navier-Stokes results in the $D_m - D_1$ plane parametrized by λ

The kinematic relation (1.13) is treated as a phase plane relation in the $D_m - D_1$ plane parametrized by λ , as in Fig. 2. The potential t -dependence of λ means that the phase orbit could wander away from the concave curves shown there. However, we wish to demonstrate certain results about the nature of solutions in different regions of this phase plane bounded by curves $\lambda = \text{const}$, so in this section λ is treated as a constant.

The curve $\lambda = 1$ is associated with the lower bound $\tilde{Q}_1 \leq \tilde{Q}_m$, which translates to

$$D_1^{\alpha_m/2} \leq D_m \quad \text{where} \quad A_{m,1} = \alpha_m/2 = \frac{m}{4m-3}. \quad (2.1)$$

Thus the regions below the line in Fig. 1 and below the curve in Fig. 2, both corresponding to $\lambda = 1$, are forbidden by Hölder's inequality. Moreover, the relation between D_m and D_1 is linear when $\lambda = 4$. The results of §2.1 alone can be found in Gibbon *et al.* (2014): the rest of the material is new.

2.1 The region $1 \leq \lambda < 2$ and the curve $\lambda = 2$

From the definition of the D_m in (1.13) note that $D_1 = L\nu^{-2}\|\omega\|_2^2$. A purely formal differential inequality for D_1 is

$$\frac{1}{2}\dot{D}_1 \leq L\nu^{-2} \left\{ -\nu \int_{\mathcal{V}} |\nabla \omega|^2 dV + \int_{\mathcal{V}} |\nabla \mathbf{u}| |\omega|^2 dV + \ell^{-1} \|\omega\|_2 \|\mathbf{f}\|_2 \right\}. \quad (2.2)$$

Dealing with the negative term first, an integration by parts gives

$$\int_{\mathcal{V}} |\omega|^2 dV \leq \left(\int_{\mathcal{V}} |\nabla \omega|^2 dV \right)^{1/2} \left(\int_{\mathcal{V}} |\mathbf{u}|^2 dV \right)^{1/2}, \quad (2.3)$$

where the dimensionless energy E is defined as

$$E = \nu^{-2} L^{-1} \int_{\mathcal{V}} |\mathbf{u}|^2 dV. \quad (2.4)$$

This is always bounded such that

$$\overline{\lim}_{t \rightarrow \infty} E \leq c Gr^2. \quad (2.5)$$

Next, the nonlinear term in (2.2) needs to be estimated. The standard result using a Sobolev inequality produces a cubic nonlinearity D_1^3 that is too strong for the negative term: all that can be deduced from this is that D_1 is bounded from above only for short times or for small initial data. The difficulty caused by this term has been known for many decades: see Constantin and Foias (1988) and Foias *et al.* (2001).

We now turn to see how the insertion of $D_m = c_{1,m} D_1^{A_{m,\lambda}}$ might mollify the nonlinear term:

$$\begin{aligned} \int_{\mathcal{V}} |\nabla \mathbf{u}| |\omega|^2 dV &= \int_{\mathcal{V}} |\omega|^{\frac{2m-3}{m-1}} |\omega|^{\frac{1}{m-1}} |\nabla \mathbf{u}| dV \\ &\leq \left(\int_{\mathcal{V}} |\omega|^2 dV \right)^{\frac{2m-3}{2(m-1)}} \left(\int_{\mathcal{V}} |\omega|^{2m} dV \right)^{\frac{1}{2m(m-1)}} \left(\int_{\mathcal{V}} |\nabla \mathbf{u}|^{2m} dV \right)^{\frac{1}{2m}} \\ &\leq C_m \left(\int_{\mathcal{V}} |\omega|^2 dV \right)^{\frac{2m-3}{2(m-1)}} \left(\int_{\mathcal{V}} |\omega|^{2m} dV \right)^{\frac{1}{2(m-1)}} \\ &= C_m L^3 \varpi_0^3 D_1^{\frac{2m-3}{2m-2}} D_m^{\frac{4m-3}{2m-2}}, \quad 1 < m < \infty. \end{aligned} \quad (2.6)$$

The penultimate line is based on $\|\nabla \mathbf{u}\|_p \leq c_p \|\omega\|_p$, for $1 < p < \infty$. Inserting the depletion $D_m = c_{1,m} D_1^{A_{m,\lambda}}$ gives

$$L\nu^{-2} \int_{\mathcal{V}} |\nabla \mathbf{u}| |\omega|^2 dV \leq c_{2,m} \varpi_0 D_1^{\xi_{m,\lambda}}, \quad (2.7)$$

where $\xi_{m,\lambda}$ is defined as

$$\xi_{m,\lambda} = \frac{A_{m,\lambda}(4m-3) + 2m-3}{2(m-1)}. \quad (2.8)$$

It can now be seen that by using (1.13), the m -dependency cancels leaving³

$$\xi_{m,\lambda} = 1 + \lambda/2. \quad (2.9)$$

³Lu and Doering (2008) showed numerically that by maximizing the enstrophy subject to $\operatorname{div} \mathbf{u} = 0$, two branches of the nonlinear term appear, the lower being $D_1^{1.78}$ and the upper $D_1^{2.997}$. Later, Schumacher, Eckhardt and Doering (2010), suggested that $7/4$ and 3 were the likely values of these two exponents: the exponent $1 + \lambda/2 = 7/4$ corresponds to $\lambda = 1.5$ which lies at the upper end of the range $1.15 \leq \lambda \leq 1.5$ observed in Gibbon *et al.* (2014).

$\xi_{m,\lambda}$ does not reach its conventional value of 3 unless $\lambda = 4$. Thus, by loading the size of D_m relative to D_1 into λ we have, in effect, made the strength of the nonlinearity dependent upon this function. (2.2) now becomes

$$\frac{1}{2}\dot{D}_1 \leq \varpi_0 \left(-\frac{D_1^2}{E} + c_{2,m}D_1^{1+\lambda/2} + GrD_1^{1/2} \right). \quad (2.10)$$

Given that E is bounded above, D_1 is always under control provided λ is restricted to the range $1 \leq \lambda < 2$. Formally, there exists an absorbing ball for D_1 of radius

$$\overline{\lim}_{t \rightarrow \infty} D_1 \leq \tilde{c}_{2,m} Gr^{\frac{4}{2-\lambda}} + O\left(Gr^{4/3}\right), \quad (2.11)$$

It has been shown in Gibbon *et al.* (2014) that this gives rise to a global attractor \mathcal{A} whose Lyapunov dimension has been estimated as

$$d_L(\mathcal{A}) \leq \begin{cases} c_{4,m} Re^{\frac{3}{5}(\frac{6-\lambda}{2-\lambda})} \\ c_{5,m} Gr^{\frac{3}{5}(\frac{4-\lambda}{2-\lambda})} \end{cases} \quad (2.12)$$

depending on whether one chooses to use the Reynolds or Grashof number.

The critical case occurs at $\lambda = 2$ but, given that $\int_0^t D_1(\tau) d\tau \leq ct Re^3$, an integration with respect to time shows that $D_1(t)$ has an exponentially growing upper bound.

2.2 The regions $2.5 \leq \lambda < 4$ and $\lambda \geq 4$

It has also been shown in Gibbon (2012) and Gibbon *et al.* (2014) that the D_m satisfy the differential inequality for $1 < m < \infty$

$$\dot{D}_m \leq D_m^3 \left(-\varpi_{1,m} \left(\frac{D_m}{D_1} \right)^{\eta_m} + \varpi_{2,m} \right) + \varpi_{3,m} Gr D_m^{1-1/\alpha_m}, \quad (2.13)$$

where $\eta_m = 2m/3(m-1)$ and where $\varpi_{1,m} < \varpi_{2,m}$ are constant frequencies. The last (forcing) term, is hard to handle in conjunction with the others so this will be separated and dealt with last: no more than algebraic growth in time can come from it. Let us now divide (2.13) by D_m^3 to obtain

$$\frac{1}{2} \frac{d}{dt} D_m^{-2} \geq \varpi_{1,m} X_m(t) D_m^{-2} - \varpi_{2,m} \quad (2.14)$$

where

$$X_m = D_m^2 \left(\frac{D_m}{D_1} \right)^{\eta_m}. \quad (2.15)$$

A bound away from zero of the time integral of $X_m(t)$ is required to show that $D_m^{-2}(t)$ never passes through zero for some range of initial conditions. To achieve this we introduce the nonlinear depletion as in (1.13). Noting that $\eta_m + 2 = 2(4m-3)/3(m-1) = 2\eta_m \alpha_m^{-1}$, it is found that ($\tilde{c}_m = c_m^{2+\eta_m}$)

$$\begin{aligned} X_m &= \tilde{c}_m D_1^{\eta_m(\lambda-1)(m-1)/m} \\ &= \tilde{c}_m D_1^{2(\lambda-1)/3}. \end{aligned} \quad (2.16)$$

It is at this point that we introduce the lower bound⁴ on $\int_0^t D_1 d\tau$ found in Doering and Foias (2002)

$$\int_0^t D_1 d\tau \geq t Gr + O(t^{-1}). \quad (2.17)$$

⁴Doering and Foias (2002) have shown that there are two estimates for the lower bound to the integral in (2.17). The first is proportional to $t Gr$ and the second to $t Gr^2 Re^{-2}$ depending on the relative sizes of the forcing length scale ℓ and the Taylor micro-scale. The first has been derived using a Poincaré inequality so it is likely to be less sharp although the two coincide when the bound $Gr \leq c Re^2$ is saturated. For simplicity we use the Gr -bound.

This comes into play only if $2(\lambda - 1)/3 \geq 1$, in which case $\lambda \geq 5/2$, where we can then use a Schwarz inequality to obtain

$$\begin{aligned} \int_0^t X_m(\tau) d\tau &\geq \tilde{c}_m \left(\int_0^t D_1 d\tau \right)^{2(\lambda-1)/3} t^{1-2(\lambda-1)/3} \\ &\geq t \tilde{c}_m Gr^{2(\lambda-1)/3} + O\left(t^{1-4(\lambda-1)/3}\right). \end{aligned} \quad (2.18)$$

(2.14) can be solved to give

$$\begin{aligned} \frac{1}{2}[D_m(t)]^2 &\leq \frac{\exp\{-\varpi_{1,m} \int_0^t X_m(\tau) d\tau\}}{\frac{1}{2}[D_m(0)]^{-2} - \varpi_{2,m} \int_0^t \exp\{-\varpi_{1,m} \int_0^\tau X_m(\tau') d\tau'\} d\tau} \\ &= \frac{\exp\{-c_m \varpi_{1,m} t Gr^{2(\lambda-1)/3}\}}{\frac{1}{2}[D_m(0)]^{-2} - \varpi_{2,m} [\tilde{c}_m \varpi_{1,m} Gr^{2(\lambda-1)/3}]^{-1} (1 - \exp\{-\tilde{c}_m \varpi_{1,m} t Gr^{2(\lambda-1)/3}\})}. \end{aligned} \quad (2.19)$$

(2.19) cannot develop a zero in the denominator if

$$D_m(0) \leq \left(\frac{1}{2} \tilde{c}_m \varpi_{1,m} \varpi_{2,m}^{-1} \right)^{1/2} Gr^{(\lambda-1)/3}, \quad (2.20)$$

for any $\lambda \geq 5/2$, in which case the solution decays exponentially. This initial data is not small but it is not huge either. The estimates above have been achieved by neglecting the forcing term in (2.14) $Gr D_m^{1-1/\alpha_m}$. The effect of the forcing term on its own yields

$$D_m \leq [\alpha_m \varpi_{3,m} Gr (t_0 + t)]^{\alpha_m}. \quad (2.21)$$

Finally, the restriction on initial data can be dropped when $\lambda \geq 4$. At $\lambda = 4$ the relation (1.14) is linear because $A_{m,4} = 1$ so $D_m = c_{1,m} D_1$ here. There is some freedom in choosing the constants $c_{1,m}$ in (1.14) : if they are chosen such that $c_{1,m}^{2+\eta_m} \geq \varpi_{1,m} \varpi_{2,m}$, the main terms in (2.13) can be dismissed except the forcing.

2.3 The region $2 < \lambda < 2.5$

The dynamics in the middle tongue-shaped region bounded by the two central curves $\lambda = 2$ and $\lambda = 2.5$ in Fig. 2 remains open. Neither the depletion of nonlinearity nor the increase in dissipation afforded by (1.14) are strong enough so we must fall back on the existence of Leray's weak solutions. The lower bound of Doering and Foias (2002) on the time integral of the enstrophy can only be used on the time integral (see (2.18))

$$\int_0^t D_1^{2(\lambda-1)/3} d\tau \quad (2.22)$$

when $\lambda \geq 2.5$. For the range $2 < \lambda < 2.5$ the dimensionless energy E can instead be used to bound (2.22) below, but if it passes close to zero for long enough, in the manner of a homoclinic orbit, then the resulting lower bound may be too small to be of use. However, (2.22) could be estimated numerically.

3 Conclusion

Subject to the closure relation (1.14), in which the effect of the higher scaled norms D_m are partly hidden in the evolution of the function $\lambda(t)$, it has been shown that the 3D Navier-Stokes equations

are regular in each of the regions when $\lambda \geq 1$ except for $2 < \lambda < 2.5$, with the proviso that initial data in the range $2.5 < \lambda < 4$ is limited. These results are summarized in Fig. 2. The two regular regions are fundamentally different. Solutions lying in the region $\lambda \geq 2.5$ seem moribund in the sense that the forcing dominates only algebraically. However, solutions in the lower region or tongue $1 \leq \lambda < 2$ live in an absorbing ball, the radius of which is given in (2.11), and it is here where all the interesting dynamics lies with a spectrum consistent with statistical turbulence theories (Frisch (1995), Doering and Gibbon (2002)). As drawn in Fig. 2 (dotted curves), the large-scale numerical simulations reported in Gibbon *et al.* (2014) lie well within this region. This is only partially satisfactory (see below) in the sense that the existence of an absorbing ball is enough for the existence of a global attractor *provided the solution trajectory remains in this region*. There are two alternatives:

1. Orbits that originate in the range $1 \leq \lambda \leq 2$ always remain there;
2. Orbits originating in the range $1 \leq \lambda \leq 2$ could travel out of this region and into the range $2 < \lambda < 2.5$.

The numerical simulations performed so far have all had their initial data resting in $1 \leq \lambda \leq 2$ and have shown no evidence for the behaviour in item 2. In fact, the observed range $1.15 \leq \lambda \leq 1.5$ indicates relatively mild dynamics. Unless a rigorous proof is found for the behaviour in item 1, the possibility that the behaviour in item 2 may occur for higher values of Re ought to be kept in mind. A series of numerical experiments are needed with initial conditions set in the four different regions which track the evolution of $\lambda(t)$. If the behaviour in item 2 is observed this would open the question of the physical manifestation of weak solutions. Given that these lack uniqueness, would there be there a corresponding physical effect, such as multiple branching of the λ -trajectories?

Acknowledgment

Thanks are due to Darryl Holm for discussions on the nature of the $\tilde{\Omega}_m$.

A The triangular Hölder inequality (1.7)

Consider the definition of Ω_m

$$L^3 \Omega_m^{2m} = \int_{\mathcal{V}} |\omega|^{2m} dV \equiv \int_{\mathcal{V}} |\omega|^{2\alpha} |\omega|^{2\beta} dV \quad (\text{A.1})$$

where $\alpha + \beta = m$. Then, for $m > 1$ and $1 \leq p \leq m-1$ and $q > 0$, we have

$$L^3 \Omega_m^{2m} \leq \left(\int_{\mathcal{V}} |\omega|^{2(m-p)} dV \right)^{\frac{\alpha}{m-p}} \left(\int_{\mathcal{V}} |\omega|^{2(m+q)} dV \right)^{\frac{\beta}{m+q}} \quad (\text{A.2})$$

where $\frac{\alpha}{m-p} + \frac{\beta}{m+q} = 1$. Solving for α, β gives

$$\alpha = \frac{q(m-p)}{p+q} \quad \text{and} \quad \beta = \frac{p(m+q)}{p+q}, \quad (\text{A.3})$$

thereby giving

$$\Omega_m^{m(p+q)} \leq \Omega_{m-p}^{q(m-p)} \Omega_{m+q}^{p(m+q)}. \quad (\text{A.4})$$

Now choose $q = 1$ and $p = m-1$ to obtain

$$\Omega_m^{m^2} \leq \Omega_1 \Omega_{m+1}^{m^2-1}, \quad (\text{A.5})$$

which leads to (1.7).

References

- [1] Broomhead, D. S., Indik, R., Newell, A. C. & Rand, D. A. (1991) Local adaptive Galerkin bases for large-dimensional dynamical systems. *Nonlinearity*, **4**, 159–197.
- [2] Constantin, P. & Foias, C. (1988) *The Navier-Stokes equations*. Chicago University Press, Chicago, USA.
- [3] Constantin P., Foias, C & Temam R. (1988) On the dimension of the attractors in two-dimensional turbulence. *Physica D*, **30**, 284–296.
- [4] Doering, C. R. & Foias, C. (2002) Energy dissipation in body-forced turbulence. *J. Fluid Mech.* **467**, 289–306.
- [5] Doering, C. R. & Gibbon, J. D. (2002) Bounds on moments of the energy spectrum for weak solutions of the 3D Navier-Stokes equations, *Physica D*, **165**, 163–175.
- [6] Donzis, D., Gibbon, J. D., Gupta, A., Kerr, R. M., Pandit, R. & Vincenzi, D. (2013) Vorticity moments in four numerical simulations of the 3D Navier-Stokes equations. *J. Fluid Mech.*, **732**, 316–331.
- [7] Donzis, D. & Yeung, P. K. (2010) Resolution effects and scaling in numerical simulations of passive scalar mixing in turbulence. *Physica D* **239**, 1278–1287.
- [8] Donzis, D., Yeung, P. K. & Sreenivasan, K. R. (2008) Dissipation and enstrophy in isotropic turbulence: scaling and resolution effects in direct numerical simulations. *Phys. Fluids*, **20**, 045108.
- [9] Escauriaza, L., Seregin, G. & Sverák, V. (2003) L^3 -solutions to the Navier-Stokes equations and backward uniqueness. *Russ. Math. Surveys* **58**, 211–250.
- [10] Farhat, A., Jolly, M. S. & Titi, E. S. (2014) *Continuous data assimilation for 2D Bénard convection through velocity measurements alone*. arXiv:1410.1767v1.
- [11] Foias, C., Jolly, M. S., Kevrekidis, I. G., Sell, G. R. & Titi, E. S. (1988) On the computation of inertial manifolds. *Phys. Lett. A*, **131**, 433–436.
- [12] Foias, C., Manley, O., Rosa, R. & Temam, R. (2001) *Navier-Stokes equations and turbulence*. Cambridge University Press, Cambridge, England.
- [13] Foias, C. & Prodi, G. (1967) Sur le comportement global des solutions non stationnaires des équations de Navier-Stokes en dimension two. *Rend. Sem. Mat. Univ. Padova*, **39**, 1–34.
- [14] Foias, C., Sell, G. R. & Temam, R. (1988) Inertial manifolds for nonlinear evolutionary equations. *J. Diff. Equ.*, **73**, 309–353.
- [15] Foias, C. & Temam, R. (1984) Determination of the solutions of the Navier-Stokes equations by a set of nodal values. *Math Comp.*, **43**, 117–133.
- [16] Foias, C. & Titi, E. S. (1991) Determining nodes, finite difference schemes and inertial manifolds. *Nonlinearity* **4**, 135–153.
- [17] Frisch, U. (1995) *Turbulence: the legacy of A. N. Kolmogorov*. Cambridge University Press.
- [18] Gibbon, J. D. (2011) A hierarchy of length scales for weak solutions of the three-dimensional Navier-Stokes equations. *Comm. Math. Sci.* **10**, 131–136.
- [19] Gibbon, J. D. (2012) Conditional regularity of solutions of the three dimensional Navier-Stokes equations and implications for intermittency. *J. Math. Phys.* **53**, 115608.
- [20] Gibbon, J. D., Donzis, D., Gupta, A., Kerr, R. M., Pandit, R. & Vincenzi, D. (2014) Regimes of nonlinear depletion and regularity in the 3D Navier-Stokes equations. *Nonlinearity*, **27**, 2605–2625.
- [21] Gibbon, J., Gupta, A., Krstulovic, G., Pandit, R., Politano, H., Ponty, Y., Pouquet, A., Sahoo, G. & Stawarz J. (2015) *Depletion of Nonlinearity in Magnetohydrodynamic Turbulence: Insights from Analysis and Simulations* – preprint.
- [22] Guckenheimer, J. & Holmes, P. (1997) *Nonlinear Oscillations, Dynamical Systems, and Bifurcations of Vector Fields*. Applied Mathematical Sciences **42**, Springer-Verlag, Berlin.
- [23] Holmes, P., Lumley, J. L. & Berkooz, G. (1996) *Turbulence, Coherent Structures, Dynamical Systems and Symmetry*. Cambridge University Press.
- [24] Ishihara T., Gotoh, T. & Kaneda, Y. (2009) Study of high-Reynolds number isotropic turbulence by direct numerical simulation. *Annu. Rev. Fluid Mech.*, **41**, 16–180.
- [25] Jones, D. A. & Titi, E. S. (1993) Upper Bounds on the number of determining modes, nodes, and volume elements for the Navier-Stokes equations. *Indiana Univ. Math. J.*, **42**, 875–887.
- [26] Kerr, R. M. (2012) Dissipation and enstrophy statistics in turbulence: Are the simulations and mathematics converging? *J. Fluid Mech.* **700**, 1–4.

- [27] Kerr, R. M. (2013) Swirling, turbulent vortex rings formed from a chain reaction of reconnection events. *Phys. Fluids* **25**, 065101.
- [28] Lu, L. & Doering, C. R. (2008) Limits on Enstrophy Growth for Solutions of the Three-dimensional Navier-Stokes Equations. *Indiana Univ. Math. J.*, **57**, 2693–2727.
- [29] Moin, P. & Mahesh, K. (1998) Direct Numerical Simulation: A Tool for Turbulence Research. *Annu. Rev. Fluid Mech.*, **30**, 539–578.
- [30] Olson, E. & Titi, E. S. (2003) Determining modes for continuous data assimilation in 2D turbulence. *J. Statist. Phys.*, **113**, no. 5-6, 799–840.
- [31] Pandit, R., Perlekar, P. & Ray, S. S. (2009) Statistical properties of turbulence: an overview. *Pramana J. Phys.*, **73**, 157–191.
- [32] Robinson, J. C. (1996) The asymptotic completeness of inertial manifolds. *Nonlinearity*, **9**, 132–1340.
- [33] Schumacher, J., Scheelb, J. D., Krasnov, D., Donzis, D., Yakhot, V. & Sreenivasan, K. R. (2014) Small-scale universality in fluid turbulence. *PNAS*, **111**, July 29, no. 30.
- [34] Schumacher, J., Eckhardt, B. & Doering, C. R. (2010) Extreme vorticity growth in NavierStokes turbulence. *Phys. Lett. A*, **374**, 861–865.
- [35] Titi, E. S. (1990) On approximate Inertial Manifolds to the Navier-Stokes equations. *J. Math. Anal. Applns*, **149**, 540–557.
- [36] Yeung, P. K., Donzis, D. & Sreenivasan, K. R. (2012) Dissipation, enstrophy and pressure statistics in turbulence simulations at high Reynolds numbers. *J. Fluid Mech.* **700**, 5–15.